Available online at www.sciencedirect.com
ScienceDirect
Trans. Nonferrous Met. Soc. China 23(2013) 1610−1616
Transactions of Nonferrous Metals Society of China
www.tnmsc.cn

Influence of rolling on internal friction peak of Mg−3Cu−1Mn alloy

Hai ZHOU[1,2], Jing-feng WANG[1,2], Fu-sheng PAN[1,2], Dan-dan XU[1,2], Ai-tao TANG[1,2], Hao LIANG[3]

1. National Engineering Research Center for Magnesium Alloys, Chongqing University, Chongqing 400044, China;
2. College of Materials Science and Engineering, Chongqing University, Chongqing 400044, China;
3. Institute of System Engineering, China Academy of Engineering Physics, Mianyang 621900, China

Received 13 February 2012; accepted 15 June 2013

Abstract: The damping capacities of as-rolled Mg−3Cu−1Mn (CM31) alloy were studied by dynamic mechanical analyses. The internal friction in the first heating shows peaks P_1, P_2 and P_3 at 118, 190, and 320 °C, respectively. The significant peak P_3, which can not be found in the cast CM31 alloy, appears in the first heating Q^{-1} curve and disappears in the second heating Q^{-1} curve. The influence of rolling on the internal friction peaks of the CM31 alloy was investigated by optical microscopy, X-ray diffraction, and electron backscatter diffraction analyses. The results show that the textures are enhanced and the twins rapidly disappear while peak P_3 appears after deformation of the CM31 alloy, and confirm that the three internal friction peaks are the dislocation damping peak, grain boundary damping peak, and the recrystallization peak caused by twins, in the as-rolled CM31 alloy.
Key words: rolling; magnesium alloys CM31; twinning; internal friction; damping capacity

1 Introduction

The modern aerospace and transportation industries are rapidly developing. Consequently, the requirements for the materials used in these fields are increasing. Such materials must have excellent mechanical and damping properties to control vibration and noise. Magnesium alloy, a promising metal material that is lightweight and has high specific strength, low density, as well as outstanding damping properties, can meet these demands [1−3]. However, it is believed that the behaviors of pure magnesium and some magnesium alloys conform with the G-L theory [4]. In this case, the damping capacity of pure Mg and its alloys has been considered to be caused by the movement of dislocations, which are weakly pinned by impurity atoms on the basal plane. However, strengthening materials traditionally involves controlled creation of internal defects and boundaries to obstruct dislocation motion. Therefore, it is hard to obtain a high-damping Mg alloy with a satisfactory strengthening effect. High-damping Mg−Zr magnesium alloys [5] are widely used, but their lower mechanical properties cannot meet the requirement of current defense and civilian industries. Other damping magnesium alloys are not mature for industrial applications, such as Mg−Si, Mg−Ni, Mg−Ca, and Mg−Cu−Mn systems. Therefore, the contradictory issues between the damping and mechanical properties of magnesium alloys urgently need to be solved.

Some studies [6,7] showed that magnesium alloys that undergo plastic deformation do not completely meet the G-L theory. Most magnesium alloys after plastic deformation develop an instability peak in the heating internal friction [8−10]. Therefore, this finding suggests that there may be other new mechanisms in the deformation of Mg alloy. The search for high-strength and high-damping magnesium alloys is gaining popularity among researchers. A new damping mechanism may be introduced to resolve the contradiction between the damping and mechanical properties, and will be greatly significant to the damping of magnesium alloys.

In the current work, Mg−3Cu−1Mn (CM31) alloys undergo single pass rolling deformation at room temperature. Then, the changes in the grain size, twins, textures, and internal friction peaks of the as-rolled CM31 alloy are studied.

Foundation item: Project (NCET-11-0554) supported by the Program for New Century Excellent Talents in University, China; Project (2011BAE22B04) supported by National Key Technology R&D Program of China; Project (51271206) supported by the National Natural Science Foundation of China
Corresponding author: Jing-feng WANG; Tel/Fax: +86-23-65112153; E-mail: jfwang@cqu.edu.cn
DOI: 10.1016/S1003-6326(13)62638-2

2 Experimental

The CM31 alloy used in the current study was melted in a steel mold (*d*80 mm) using an induction furnace under atmosphere of argon gas. The alloy was cooled in air after adequate stirring. The chemical composition of the cast CM31 was Mg−2.8Cu−0.7Mn (mass fraction, %), named as CM31-0% in this work. The CM31 ingot was homogenized at 380 °C for 12 h, and was made into plates of 8.5 mm in thickness and 64 mm in width. These plates were rolled by a single-pass process at a speed of 0.186 m/s and a rolling reduction of 4.7% at room temperature, named as CM31-4.7%. The specimens for the dynamic mechanical analysis (DMA) experiments were cut from the as-rolled plate vertically along the rolling direction. The dimensions of the specimen were 40 mm×5 mm×1.2 mm. The Q^{-1} values of the specimens were determined using a TA Q800 DMA equipment configured with a single cantilever. Each DMA specimen was heated from 30 °C to 400 °C at a constant heating rate of 5 °C/min. The testing frequency and strain amplitude were set at 1 Hz and 5×10^{-4}, respectively.

The tests were interrupted at each peak temperature during the DMA heating tests, and the specimen was in-situ cooled for understanding the origin of each peak appearance. The samples for microstructural observation were prepared by the standard metallographic procedure using an etching solution containing 3 g of picric acid dissolved in 20 mL of acetic acid, 20 mL of demonized water, and 100 mL of alcohol. The textures and twins of these as-quenched samples were investigated by X-ray diffraction (XRD) and electron backscatter diffraction (EBSD) tests. XRD measurements were done on the equipment of Rigaku 2500/pc using Cu K_α radiation at a scanning rate of 4 (°)/min from 10° to 90°. EBSD measurements were performed using a scanning electron microscope with a scanning step size of 1 and a magnification of 200. The specimens were electro-polished in ACII prior to EBSD experiments. The time and voltage were set to 50 s and 20 V, respectively. Finally, the samples for each test were all collected from the core of the materials to guarantee experimental accuracy.

3 Results and discussion

3.1 Heating Q^{-1} spectrum

Figure 1 shows the heating Q^{-1} spectra of CM31 alloy. As shown in Fig. 1(a), the spectrum of as-cast CM31 alloy exhibits peaks P_1 and P_2 at 73.6 and 202 °C, respectively. However, there are three peaks, namely, P_1, P_2, and P_3, whose temperatures are 118, 190, and 320 °C, respectively, in the spectrum of CM31 after rolling (that was called CM31-4.7%-I in the following paragraphs), as shown in Fig. 1(b). The damping capacity of the as-rolled CM31 alloy is lower than that of the as-cast CM31 alloy in the temperature range of 30 °C to 200 °C. Figure 1(c) shows the second heating Q^{-1} spectrum of the as-rolled CM31, named CM31-4.7%-II. All three internal friction peaks have been changed, especially P_3, which is suppressed and becomes quite inconspicuous. The temperatures of each peak are 65, 163, and 316 °C, respectively. Table 1 summarizes the information from the spectra of three states of the alloy CM31.

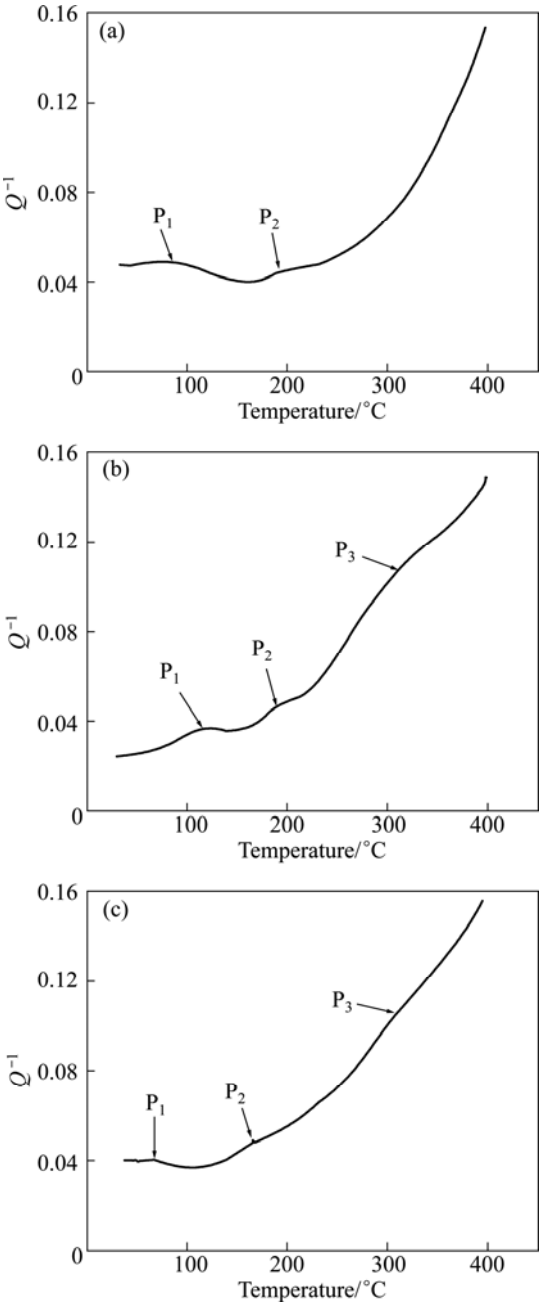

Fig. 1 Temperature—damping curves of CM31 alloys: (a) CM31-0% alloys in annealed state; (b) First heating, rolled CM31-4.7% alloy; (c) Second heating, rolled CM31-4.7% alloy

Table 1 Feature of peaks in CM31 alloys with different treatments

State	Peak P_1	Peak P_2	Peak P_3
CM31-0%	73.6 °C, conspicuous	202 °C, conspicuous	None
CM31-4.7%-I	118 °C, conspicuous	190 °C, conspicuous	320 °C, conspicuous
CM31-4.7%-II	65 °C, conspicuous	163 °C, inconspicuous	316 °C, inconspicuous

3.2 Microstructures

To observe appearance and disappearance of peak P_3, the tests were interrupted at each peak temperature during the DMA heating tests and then the specimen was rapidly cooled. Thereafter, the quenched specimens were subjected to XRD and EBSD tests, as well as microstructural observation to analyze the influence factors of P_3. Figure 2 shows the optical micrographs of CM31 alloy after different treatments. The secondary dendrite arm spacing (SDAS) of the samples changes with different treatment processes, as shown in Table 2. In the micrographs of the samples, there are numerous dendrites caused by long annealing. There is almost no change for the dendrites after minor deformation.

Table 2 Secondary dendrite arm spacing (SDAS) of CM31-4.7% samples with different treatments

Sample	Heating process	SDAS/μm
CM31-0%	−	195.7
CM31-4.7%	−	182.6
	Quenching at 120 °C	177.3
	Quenching at 190 °C	163.2
	Quenching at 320 °C	161.7
	Furnace cooling from 320 °C	180.1

As shown in Figs. 2(a) and (b) as well as Table 2, a small number of grains may exhibit breakage of CM31 alloy during the rolling at room temperature, resulting in a small secondary dendrite arm spacing, although the change is not significant. The secondary dendrite arm spacing of the as-quenched samples gradually becomes smaller with increasing temperature. Recrystallization

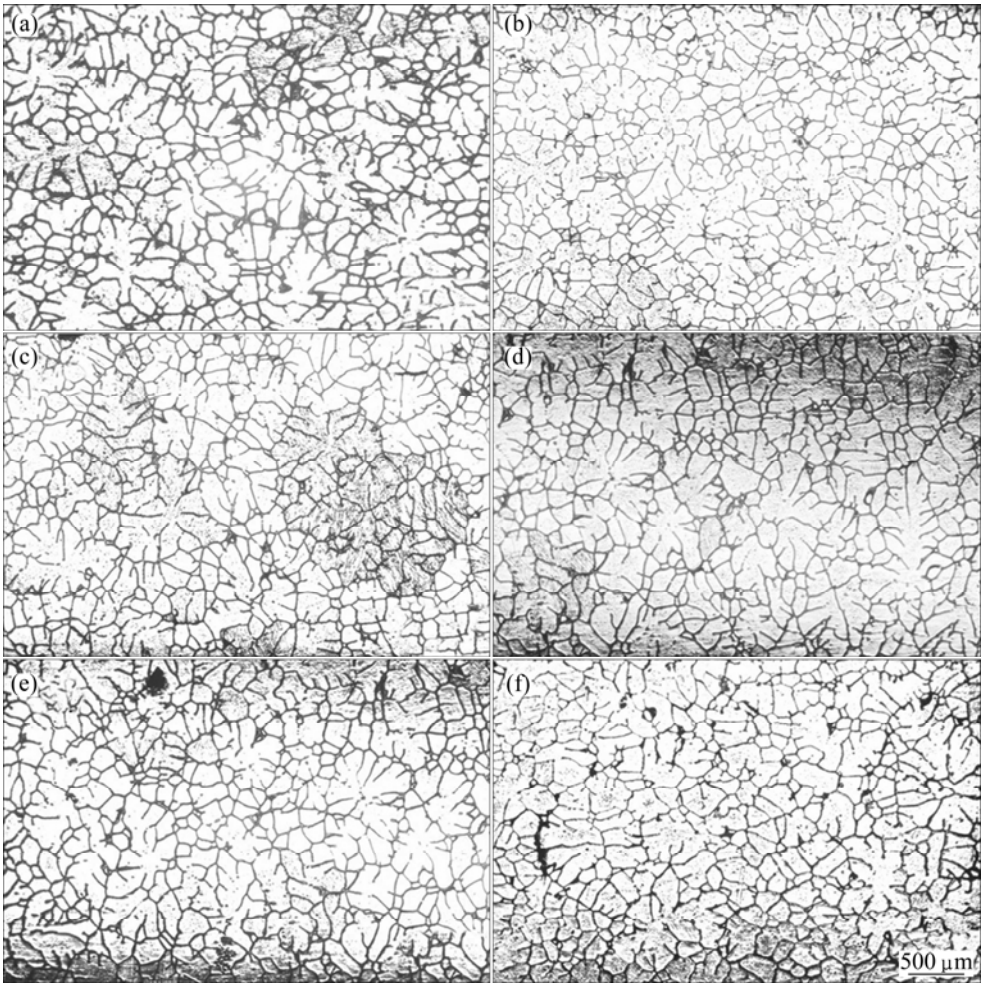

Fig. 2 Microstructures of CM31-4.7% samples with different treatments: (a) Before rolling; (b) After rolling; (c) Quenching at 120 °C; (d) Quenching at 190 °C; (e) Quenching at 320 °C; (f) Furnace cooling from 320 °C

occurs in the DMA test when the specimen was warming from 30 °C to 400 °C at a rate of 5 °C/min [11,12]. The grain growth and secondary dendrite arm spacing become larger during furnace cooling from 320 °C, as shown in Figs. 2(c), (d), (e), and (f), as well as Table 2.

3.3 Textures

The XRD patterns of the samples are shown in Fig. 3. The intensity ratio of the first three strong peaks is given by $\eta_1=I_{(101)_{Mg}}/I_{(100)_{Mg}}$ and $\eta_2= I_{(101)_{Mg}}/I_{(201)_{Mg}}$. Plastic deformation and heat treatment can change the texture in magnesium alloys, so the typical base surface textures are enhanced during rolling and are altered during the heating DMA tests [13−15]. η values of the heat-treated samples are shown in Table 3. η_1 is 2.04 at the rolled state, and it changes to 5.52 and 2.79 after quenching at 190 °C and 320 °C, respectively. For the sample air cooled at 320 °C, η_1 reaches 2.98 and almost does not change. η_2 becomes to be 5.52 and 2.79 after quenching at 190 °C and 320 °C, respectively, while it is 2.25 at the rolled state. These data suggest that texture development is caused by recrystallization-preferred growth [16].

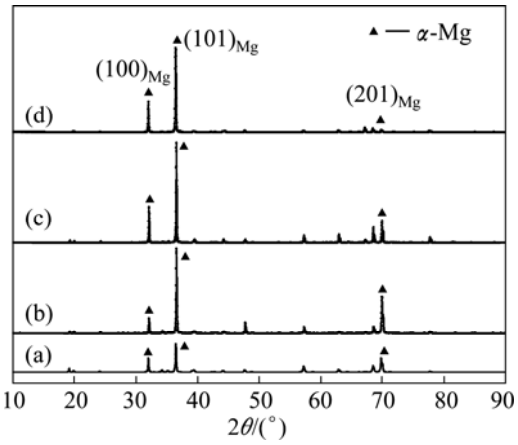

Fig. 3 XRD patterns of samples with different treatments: (a) Rolling state; (b) Quenching at 190 °C; (c) Quenching at 320 °C; (d) Furnace cooling from 320 °C

Table 3 XRD peak intensity of heat-treated samples

Peak	Peak intensity			
	Rolling state	Quenching at 190 °C	Quenching at 320 °C	Furnace cooling from 320 °C
$(101)_{Mg}$	8083	24 239	28 784	23 667
$(100)_{Mg}$	3959	4390	10321	7948
$(201)_{Mg}$	3590	10452	6352	568
η_1	2.04	5.52	2.79	2.98
η_2	2.25	2.32	4.53	41.67

3.4 Twin distribution

Figure 4 shows the results of the EBSD tests, revealing the twinning mechanism of CM31 during rolling at room temperature. The twins form an 86° angle with the major matrix produced during the rolling for a small deformation [17]. The red needle in Fig. 4 is tensile twins. Figure 4(a) shows that all grains have tensile twins, some of which are densely distributed in the upper left corner. There are still a large number of twins in the matrix of the sample quenched at 220 °C, whereas most disappear in the sample quenched at 320 °C for static recrystallization. The EBSD tests indicate that the twins are developed during recrystallization, and their significant change is closely related to the occurrence of the peak P_3.

4 Discussion

Peak P_1 in the heating Q^{-1} curve of pure magnesium and magnesium alloys is believed to be associated with the movement of dislocation [7]. As shown in Fig. 1(a), the peak P_1 in the heating Q^{-1} curve of as-cast CM31 alloy appears at a relatively low temperature of about 73.6 °C, which conforms with the result of HU et al [8,9], who pointed out that the dislocation damping peak of as-cast pure magnesium, Mg−Ni, and Mg−Si alloys occurs at about 80 °C. However, the peak P_1 occurs at 118 °C in the first heating Q^{-1} curve of rolling-state CM31-4.7% alloy. After deformation, the temperature of peak P_1 is changed. And the grain size trails off as the grains are broken down. The dislocations entangle in this alloy during the deformation at room temperature, and the dissolution of dislocation entanglement requires high activation energy. Simultaneously, the damping properties of the as-rolled CM31 alloy are lower than those of the as-cast CM31 alloy in the temperature range of 30 °C to 200 °C, as shown in Fig. 1(b). During DMA test, the temperature reaches 400 °C and stays at such high temperatures for a long time, so the test takes a similar role as heating. Therefore, the grain of the rolled alloy grows and the entangled dislocation solute in the second heating Q^{-1} curve of the rolling-state CM31-4.7% alloy becomes the straight and moving dislocation, leading to the recovery of damping properties. The temperature of peak P_1 in the second heating Q^{-1} curve of the rolling-state CM31-4.7% alloy returns to 65 °C. The shape of peak P_1 in the CM31-4.7%-II curve becomes similar with that of the CM31-0% curve.

The peak P_2 in the heating Q^{-1} curves of CM31-0% and CM31-4.7%-I have the same shape and relatively narrow temperature ranges (202 and 190 °C, respectively). MUNITZ et al [18] found that a Q^{-1} peak appears between 150 °C to 200 °C in the heating Q^{-1} curve of as-cast pure magnesium and inferred that it was the grain boundary peak. The peak has obvious characteristics of thermal activation, and its activation energy was calculated as 1.39 eV. WANG [19]

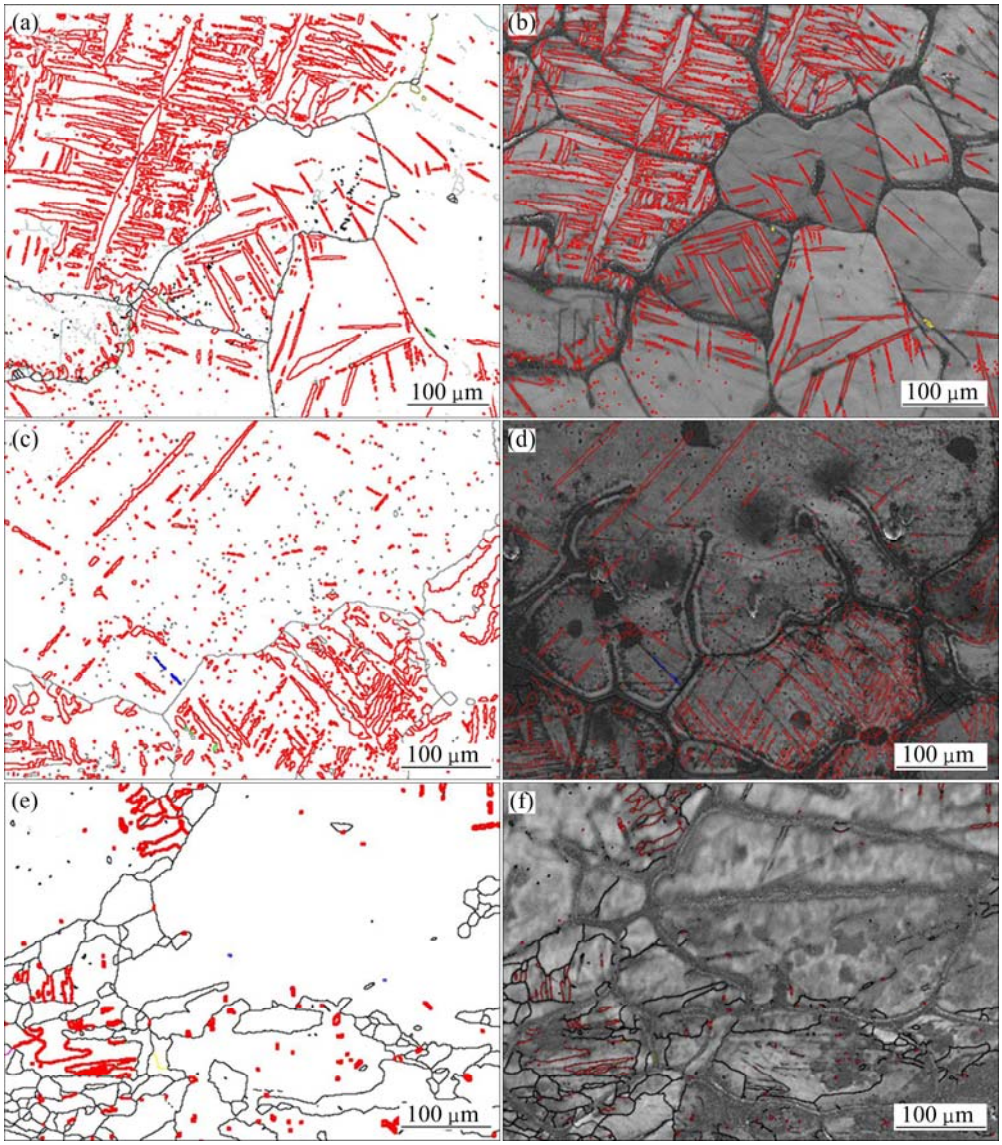

Fig. 4 EBSD images of CM31-4.7% samples with different treatments: (a), (b) CM31-4.7%; (c), (d) Quenching at 220 °C; (e), (f) Quenching from 320 °C

discovered the same phenomenon in the as-rolled Mg-3%Al alloy. Therefore, the peak P_2 in the present experiment may also be the grain boundary damping peak. The peak P_2 in the curve of CM31-0% emerges at a higher temperature (202 °C). Hence, this phenomenon is caused by numerous dendrites, which are stable and difficult to slip in the samples. However, after the rolling deformation, some grains break down and many tensile twins generate, which are high-angle grain boundaries and relatively easy to slide. The grain boundaries change from the equilibrium to non-equilibrium, so the stored grain boundary energy is increased and the activation energy is decreased [20,21]. Considering all these factors, the peak shape becomes apparent and the temperature of peak P_2 decreases in the curve of CM31-4.7%-I.

In the present study, a significant peak P_3 appears in the first heating Q^{-1} curve, and disappears in the second heating Q^{-1} curve of the as-rolled CM31 alloy. A number of researchers are interest in the unstable internal friction peak P_3. XIAO [22] researched AZ31 after plastic deformation, and found that peak P_3 is related to the stored energy at 200 and 250 °C after the low- and high-temperature deformation of ECAP, respectively, and the peak disappears during the heating process. WANG [19] analyzed the heating Q^{-1} curve of as-rolled Mg−3%Al alloy, and concluded that peak P_3 at 300 °C to 350 °C does not shift with the change in frequency. The temperature of peak P_3 decreases with the increasing amount of pressure, increases during the heating process, and is more difficult to produce when being fully annealed. And he inferred that P_3 of as-rolled Mg−3%Al is a recrystallization peak. WU et al [23] surmised that

peak P_3 of as-heat-rolled Mg−Li alloy is related with textures. These textures are significantly enhanced with increasing temperature during the DMA test. The XRD analyses in the present study revealed the similar results. The alloy undergoes initial recrystallization, which does not fundamentally change the texture during the first DMA test. The intensity of the textures changes because the recrystallized grains prefer growth [24,25]. Compared with the rolled alloy, η_1 changes from 2.04 to 5.52 and 2.79 at 220 and 320 °C, respectively. η_2 has the similar result with η_1. The intensity of the textures gradually increases, as shown in Fig. 3 and Table 3. Combined with EBSD tests, the alloy produces a large number of tensile twins that form an 86° angle with the matrix after minor deformation. There are also still a large number of twins in the matrix at the P_2 temperature (220 °C), whereas most disappear at the P_3 temperature (320 °C) in the static recrystallization during the first heating DMA test. Peak P_3 is completely suppressed and becomes inconspicuous in the second heating DMA test. Therefore, peak P_3 forms as a result of the disappearance of most twins and change in texture due to static recrystallization to exhaust a large amount of energy. Most twins disappear at peak P_3 temperature, and subsequently, a large amount of energy is consumed. Therefore, peak P_3 is inhibited and becomes very inconspicuous in the CM31-4.7%-II curve.

5 Conclusions

1) After rolling deformation at room temperature, a large number of tensile twins are densely distributed in the grain, and the base surface texture is obtained. Three peaks, namely, P_1, P_2, and P_3, appear in the first heating Q^{-1} curve of as-rolled CM31 alloy. Compared with the cast CM31 alloy, the significant peak P_3 appears in the first heating DMA test, and disappears in the second heating DMA test.

2) Combined with the previous reports, the variations in peak P_1 can be attributed to the impact of rolling to the dislocation and peak P_2 is grain boundary damping peak.

3) Most twins rapidly disappear and the textures are enhanced during static recrystallization, while the peak P_3 becomes quite inconspicuous. Therefore, peak P_3 results from the disappearance of twins and the change in textures.

References

[1] ZHANG Zhen-yan, PENG Li-ming, ZENG Xiao-qing, DING Wen-jiang. Effects of Cu and Mn on mechanical properties and damping capacity of Mg−Cu−Mn alloy [J]. Transactions of Nonferrous Metals Society of China, 2008, 18: 55−58.

[2] WANG Jian-qiang, QI Hai-bo, ZHU Hao, GUAN Shao-kang, YU Xu-guang, FAN Yun-chang. A study of the effect of antimony content on damping capacity of ZA84 magnesium alloy [J]. Mater Des, 2011, 32: 4567−4572.

[3] WAN Di-qing, WANG Jin-cheng, WANG Gai-fang, CHEN Xian-yi, LIN Lin, FENG Zhi-gang, YANG Gen-cang. Effect of Mn on damping capacities, mechanical properties, and corrosion behaviour of high damping Mg−3 wt.%Ni based alloy [J]. Mater Sci Eng A, 2008, 494: 139−142.

[4] GRANATO A, LUCKE K. Theory of mechanical damping due to dislocations [J]. J Appl Phys, 1956, 27: 583−593.

[5] WANG J F, SONG P F, GAO S, HUANG X F, SHI Z Z, PAN F S. Effects of Zn on the microstructure, mechanical properties, and damping capacity of Mg−Zn−Y−Zr alloys [J]. Mater Sci Eng A, 2011, 528: 5914−5920.

[6] NISHIYAMA K, MATSUI R, IKEDA Y, NIWA S, SAKAHUCHI T. Damping properties of a sintered Mg−Cu−Mn alloy [J]. J Alloys Compd, 2003, 355: 22−25.

[7] ZHENG Ming-yi, FAN Guo-dong, TONG Li-bo, HU Xiao-shi, WU Kun. Damping behavior and mechanical properties of Mg−Cu−Mn alloy processed by equal channel angular pressing [J]. Transactions of Nonferrous Metals Society of China, 2008, 18: 33−38.

[8] HU Xiao-shi, WU Kun, ZHENG Ming-yi. Low frequency damping capacities and mechanical properties of Mg−Si alloys [J]. Mater Sci Eng A , 2007, 452: 374−379.

[9] HU Xiao-shi, WU Kun, ZHENG Ming-yi. Effect of heat treatment on the stability of damping capacity in hypocutectic Mg−Si alloy [J]. Scripta Mater, 2006, 54: 1639−1643.

[10] WATANABE H, MUKAI T, SUGIOKA M, ISHIKAWA K. Elastic and damping properties from room temperature to 673 K in an AZ31 magnesium alloy [J]. Scripta Mater, 2004, 51: 291−295.

[11] XU Z, TANG G, DING F, TIAN S, TIAN H. The effect of multiple pulse treatment on the recrystallization behavior of Mg−3Al−1Zn alloy strip [J]. Appl Phys A, 2007, 88: 429−433.

[12] MARTINEZ O E, ARCHIOPOLI U C, CESA Y, MINGOLO N. Crystallization of glassy metal surfaces in Mg−Zn alloy determined by resonant photoacoustic detection [J]. Appl Phys A, 2005, 81: 1667−1674.

[13] LIU Qing. Research progress on plastic deformation mechanism of Mg alloys [J]. Acta Metallurgica Sinica, 2011, 46(11): 1458−1472. (in Chinese)

[14] SUN Hong-fei, LIANG Shu-jing, WANG Er-de. Mechanical properties and texture evolution during hot rolling of AZ31 magnesium alloy [J]. Transactions of Nonferrous Metals Society of China, 2009, 19: 349−354.

[15] XIA M X, ZHENG H X, YUAN S, LI J G. Recrystallization of preformed AZ91D magnesium alloys in the semisolid state [J]. Mater Des, 2005, 26: 343−349.

[16] TANG W N, CHEN R S, ZHOU J, HAN E H. Effects of ECAE temperature and billet orientation on the microstructure, texture evolution and mechanical properties of a Mg−Zn−Y−Zr alloy [J]. Mater Sci Eng A, 2009, 499: 404−410.

[17] SONG G S, ZHANG S H, ZHENG L, RUAN L Q. Twinning, grain orientation and texture variation of AZ31 Mg alloy during compression by EBSD tracing [J]. J Alloys Compd, 2011, 509: 6481−6488.

[18] MUNITZ A, DAYAN D, RICKER R. Dynamic mechanical analysis of pure Mg and AZ31 alloy [J]. Magnesium Technology, 2004, 12: 103−106.

[19] WANG Shi-cun. Effect of rolling process on damping capacity and mechanical properties of Mg−3%Al alloy [D]. Harbin: Harbin Institute of Technology, 2009: 46−56. (in Chinese)

[20] DUDAREV E F, POCHIVALOVA G P, KOLOBOW Y R. True grain-boundary slipping in coarse and ultrafine-grained titanium [J]. Russian Physics Journal, 2004, 47: 617−625.
[21] MULYUKOV R R, AKHMADEEV N A, VALIEV R Z. Strain amplitude dependence of internal friction and strength of submicrometre-grained copper [J]. Mater Sci Eng A, 1993, 171: 143−149.
[22] XIAO Kai. The effect of ECAP deformation on mechanical property and damping capacity of AZ31 magnesium alloy [D]. Harbin: Harbin Institute of Technology, 2007: 55−64. (in Chinese)
[23] WU S K, CHANG S H, TSIA W L, BOR H Y. Low-frequency damping properties of as-extruded Mg−11.2Li−0.95Al−0.43Zn magnesium alloy [J]. Mater Sci Eng A, 2011, 528: 6020−6025.
[24] YANG Ping, RENG Xue-ping, ZHAO Zu-de. Microstructures and textures in hot deformed and annealed AZ31 magnesium alloy [J]. Transactions of Metal Heat Treatment, 2003, 24(4): 12−16. (in Chinese)
[25] AGNEW S R, DUYGULU. Plastic anisotropy and the role of non-basal slip inmagnesium alloy AZ31B [J]. International Journal of Plasticity, 2005, 21: 1161−1193.

轧制对 Mg−3Cu−1Mn 合金温度阻尼峰的影响

周 海[1,2]，王敬丰[1,2]，潘复生[1,2]，徐丹丹[1,2]，汤爱涛[1,2]，梁 浩[3]

1. 重庆大学 国家镁合金工程技术研究中心，重庆 400044；
2. 重庆大学 材料科学与工程学院，重庆 400044；
3. 中国工程物理研究院 总体工程研究所，绵阳 621900

摘 要：经过变形量 4.7%的单道次室温轧制变形，Mg−3Cu−1Mn 合金的一次温度—阻尼谱出现了 3 个明显的阻尼峰；在二次温度—阻尼谱中，3 个阻尼峰均发生变化，特别是第 3 阻尼峰 P_3 受到抑制，变得非常不明显。对各阻尼峰峰温处淬火样品进行金相、XRD、EBSD 等实验，研究轧制对 Mg−3Cu−1Mn 合金温度—阻尼峰的影响。结果表明：在一次温度—阻尼谱中的 P_3 峰处出现织构增强、孪晶急剧消失的现象；轧制变形后，3 个温度—阻尼峰依次为位错阻尼峰、晶界阻尼峰和孪晶引发的再结晶阻尼峰；另外，随着拉伸孪晶的消失，室温轧制态 Mg−3Cu−1Mn 合金的应变阻尼性能大幅度恢复，高应变下接近均匀化退火态 Mg−3Cu−1Mn 的应变阻尼性能。这说明拉伸孪晶对 Mg−3Cu−1Mn 合金应变阻尼性能有不利的影响。

关键词：轧制；镁合金 CM31；孪晶；内耗峰；阻尼

(Edited by Sai-qian YUAN)